DFT Study on Metamagnetics β-$M(OH)_2$ (M = Mn, Fe, Co, Ni)

IOP Conf. Series: Journal of Physics: Conf. Series **1247** (2019) 012046 doi:10.1088/1742-6596/1247/1/012046

DFT Study on Metamagnetics β-$M(\mathrm{OH})_2$ (M = Mn, Fe, Co, Ni)

A. C. Garcia-Castro[1], R. Ospina[1], A. H. Romero[2]

[1]Department of Physics, Universidad Industrial de Santander, Carrera 27 Calle 9, 680002, Bucaramanga, Colombia.
[2]Department of Physics and Astronomy, West Virginia University, WV-26506-6315, Morgantown, USA.

E-mail: acgarcia@uis.edu.co

Abstract. First-principles calculations have been carried out in order to analyze the structural, vibrational, and magnetic properties in the A-type antiferromagnetic (AFM) β-$M(\mathrm{OH})_2$ metal transition hydroxides. Theoretical results demonstrate a quasi layer-by-layer magnetic behavior with strong ferromagnetic (FM) interactions in the intralayer plane and weak AFM behavior between the interlayer. This behavior corresponds to an A-type AFM behavior for β-$M(\mathrm{OH})_2$ (M = Mn, Fe, Co, and Ni) with energy differences around 3.0 meV with respect to the FM state. Structural analysis reveal a clear influence of Van der Waals (VdW) interactions in the stabilization of the phase giving high accuracy in lattice parameter when compared to experimental findings. Qualitative analysis of the magnetic exchange interactions reveals a higher exchange intralayer interaction for M = Ni, and higher exchange or dipolar interlayer interactions for M = Mn. Vibrational analysis, in the M = Ni case, demonstrate a correct IR and Raman modes assignments according to experimental results on the $P\bar{3}m1$ space group.

1. Introduction

Magnetic $M(\mathrm{OH})_2$ hydroxides are well known systems that recently have attracted new perspectives and their properties are been revised [1, 2]. Experimental analysis and reports have shown that these magnetic materials exhibit a layered structure based-on metal transition hydroxides ($M(\mathrm{OH})_2$, M = Mn, Fe, Co, and Ni). From the experimental point of view, the magnetic behavior of $\mathrm{Mn(OH)_2}$ [3], $\mathrm{Fe(OH)_2}$ [4], $\mathrm{Co(OH)_2}$ [5], and more recently $\mathrm{Ni(OH)_2}$ [1, 2] compounds have been studied. It has been found that these materials present a strong ferromagnetic intralayer interaction and weak antiferromagnetic interaction between the interlayers. Additionally, in M = Co and Ni, the metal hydroxides exhibit a magnetic ordering phenomena known as metamagnetism, where the antiferromagnetic ground state is changed to ferromagnetic one through the application of an external magnetic field. This transition is totally different from a second-order transition induced by a temperature change (*i.e.* antiferromagnetic to paramagnetic) defined as Néel temperature ($\mathrm{T_N}$). This difference in the magnetic behavior makes these layered materials of large interest. Additionally, this family of materials presents an interesting superexchange and dipolar interactions phenomena for interlayer and intralayer that are not well understood [6]. Thus, the magnetic exchange interactions between layers remain unclear and the theoretical phenomena that could lead to this behavior has not been clarified.

In order to shed some light into the magnetic ordering and structural behavior in these metal transition hydroxides with special focus in $Ni(OH)_2$ and β-phases, we have performed a series of first-principles DFT based studies for the hexagonal structure of these compounds with $P\bar{3}m1$ (164) space group .

2. Computational Details

First-principles calculations have been performed within Density Functional Theory (DFT) as implemented in the Vienna Ab-initio Simulation Package (VASP) [7, 8]. Projector Augmented Wave (PAW) [9] pseudo-potentials were used to represent the valence and core electrons. The electronic configuration taken into account in pseudo-potential as valence electrons were 13 for Mn ($3p^6 3d^5 4s^2$), 13 for Fe ($3p^6 3d^6 4s^2$), 9 for Co ($4s^2 3d^7$), 16 for Ni ($3p^6 3d^8 4s^2$), 6 for O ($2s^2 2p^4$) and 1 for H ($1s^1$). The exchange correlation will be represented within the General Gradient Approximation (GGA) and Perdew-Burke-Ernzerhof for Solids (PBEsol) parametrization [10]. Due to the magnetic character of these systems, we need to include the spin in the calculation and make the proper use of the exchange correlation (LSDA). The correction due to the large d-electron localization by means of the LDA+U method (GGA+U, U = 4 eV, J = 0 eV) was taken into account. The periodic solution of these crystalline structures will be represented by using Bloch states with a k-point mesh of (6×6×6) centered at the Γ-point and 1400 eV energy cut-off, which has been tested already to give forces convergence to less than 0.01 eV/A and an error in total energy around ± 0.4 meV. Due to the layered configuration of this material, it is expected that Van der Waals forces will play an important role. Therefore, we take them into account by including them into the calculation, by using the semi-empirical method developed by Grimme [11]. The optimized structure will be compared with the obtained XRD measurements. Phonons are calculated by using the frozen phonon approach, which relies in calculating the dynamical matrix constant from the super cell and mapped to the unit cell.

3. Results and Discussion

A hexagonal structure of the metal transition-hydroxides (see Figure 1) with A-type antiferromagnetic order was found in full agreement with experimental reports. The obtained lattice parameters, a and c give us an error around 0.6% and 2.0% with respect to the reported experimental values [1]. This difference on the c parameter in all the structures suggest a strong presence of Van der Waals (VdW) interactions along c-axis, as expected. After taking into account the VdW interaction into the calculations, the error on the c lattice parameter was reduced to approx. 0.6 %, which is a strong evidence of the effect of this interaction in the formation of the layered lattice structure. Figure 1 shows the XRD patterns for β-phase. The structure and patterns are in full agreement with the experimentally reported by Rall *et al.* for M = Ni [1]. A shift to higher 2θ degrees values reveals the expected contraction in the a and c lattice parameters as a function of the atomic radius observed for the metal transition cations when going from Mn to Ni. Interestingly enough, even though VdW interaction does not give any electronic transfer, it will create a confinement due to the layer proximity, which we believe, it is responsible of changes in the magnetic properties. Additionally, exchange and dipolar magnetic interactions are very sensitive to M-M distance.

A-AFM and FM states were tested in order to determine the magnetic ground state for hydroxides. The differences in energy ($\triangle E = E_{AFM} - E_{FM}$) found were -4.5, -3.3 and 4.2 meV for Mn, Fe, and Ni respectively. Contrary to experimentally reported, the difference in the magnetic ground state energy for M = Co, was positive, which could suggest a ferromagnetic ground state for $Co(OH)_2$.

The magnetic moment values per cation were 4.6, 3.7, 2.7 and 1.7 μ_B for Mn, Fe, Co, and Ni respectively. These values are in full agreement with experimental reports for Fe and Mn [4][12]. Moreover, are the expected magnetic moments due to the d-level filling, having the higher value

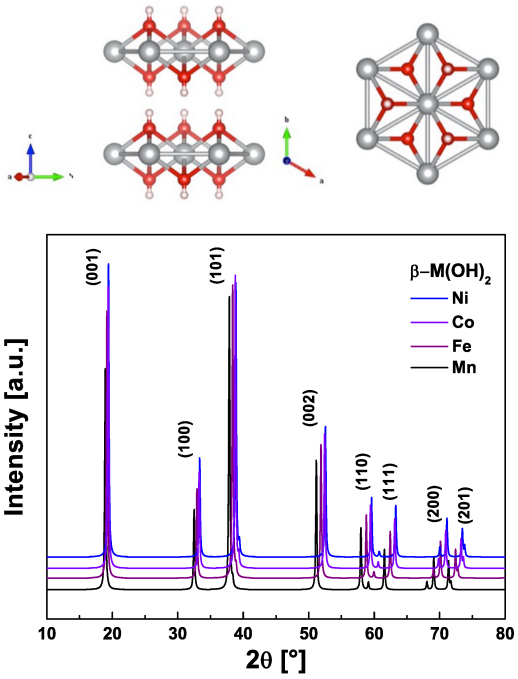

Figure 1. On the top, hexagonal $P\bar{3}m1$ structure with M atoms in grey, O in red, and H in light rose. On the bottom, XRD simulated patterns for β–$M(\mathrm{OH})_2$ (M = Mn, Fe, Co, Ni).

for Mn^{+2} with five unpaired electrons and the lowest one for Ni^{+2} with two unpaired electrons according to Hund's rule.

The analysis on the total electronic density (ED) and the electron localized function (ELF) images along the (110) plane (in Figure 2), as well as the electronic density of states (in Figure 3), reveal a clear covalent bonding interaction between O–H, as expected. We also note the presence O:$2p$ – M:$3d$ hybridization, as confirmed in the ED image for O–M bonding zone. This interaction could enhance the expected magnetic properties within this system. The ELF at (001) (not shown here) also demonstrate a delocalized electrons characteristic of metallic bonding as expected in the M-layers. Localized electrons or electronic density localized between layers were not found, which is the evidence of weak interaction between layers making more important the VdW interactions as commented before.

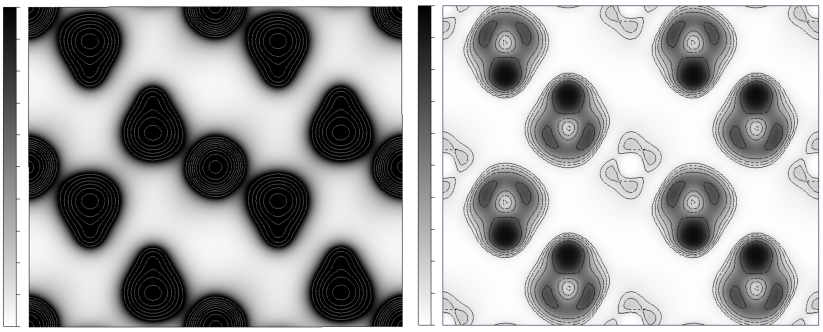

Figure 2. On the right, total electronic density in (110) plane. On the left, electron localized functions (ELF) in (110) plane (scale from 0 to 1).

Local density of states (L-DOS in Figure 3) show the AFM populations of states, with a total cancellation of magnetization as expected. The electronic gap increase as a function of *d*-level fill from Fe to Ni, as expected according to *d*-level fill in these tetragonal crystal field splitting configurations for M-O_6. Electronic gap of $E_g = 2.9$ eV was found for M = Ni in well agreement with experimental reported [13, 14] measured by UV spectroscopy taking a value between 3.0 to 3.5 eV. Additionally, it is observed an overlapping between the M:3*d* and the O:*p*, in agreement with the ED and ELF images analysis presented above. From Figure 3 it is also noted that the M–O bonding interaction is higher for M = Fe in comparison with Mn, Co, and Ni. The latter could lead to a strongest magnetic superexchange interaction for the intralayer zone in the Iron-based hydroxide. On the other side, $Mn(OH)_2$ shows a large gap value ($E_g = 2.8$ eV) than the expected from the trend. This effect could be induced by the change in the *d*-level fill. In the Mn case, its *d*-orbital is totally filled with unpaired electrons but immediately later, for the Fe case, the electrons in its *d*-orbital begin to be paired reducing then, the gap energy.

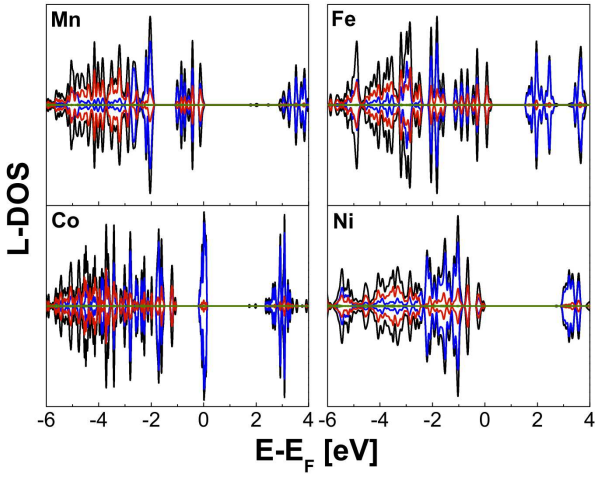

Figure 3. Local-DOS for β–$M(OH)_2$ showing an AFM behavior of this phase. In black the total DOS, in blue the M:3*d*-levels, in red the O:2*p*-levels, and in green, the H:1*s*-levels

On the vibrational side, based-on the group symmetry, the group representation for this hexagonal structure with $P\bar{3}m1$ space group is given by [15]:

$$\Gamma = 2A_{1g} \oplus 2E_g \oplus 2A_{1u} \oplus 2E_u \quad (1)$$

The phonon modes for $Ni(OH)_2$ are reported in Table 1. These have been calculated by considering the final optimized geometry, where the Van der Waals correction has been included. The phonon-dispersion calculations for this phase (not presented here) show clearly that this phase is thermally stable with all phonon frequencies positive at Γ point. However, a small negative band in *K*-point suggest small thermal and structural fluctuations, an observation noticed previously, as in the $Mg(OH)_2$ compound [16]. To the best of our knowledge, these thermal fluctuations do not affect the analysis presented here. The Raman and IR modes for $Ni(OH)_2$ were identified and compared with the experimental reports of Murli *et al.* [14] and Bantignies *et al.* [13] showing an excellent agreement as we can see in Table 1.

In order to analyze the magnetic behavior for the intralayer and interlayer regimes in the hydroxides we studied the magnetic interactions in the structure. According to T. Enoki *et al.* [12] the exchange and dipolar interactions in this system consist of three components for the first, second and third neighbors respectively. For those interactions, the exchange constants

Raman modes		
Mode	[cm^{-1}] Murli et al. [14]	[cm^{-1}] present work
A_{1g}	325	329
E_g	450	448
E_g	880	860
A_{1g}	3580	3702
IR modes		
Mode	[cm^{-1}] Bantignies et al [13]	[cm^{-1}] present work
E_u	332	331
A_{1u} or E_u	440	443
A_{1u}or E_u	530	505
A_{1u}	3636	3715

Table 1. Phonons at Γ-point in the β-Ni(OH)$_2$ phase: Raman and IR are compared directly with experimental results [14, 13].

have been classified according to the neighborhood, then, J_1 is the intralayer magnetic interaction which occur between M–M indirect path through two oxygen bondings and can be classified as superexchange interaction. The J_2 and J_3 exchange constants lie in the interlayer interaction. In the Ni(OH)$_2$ case, the exchange constants have been experimentally obtained [1] and it was found a strong ferromagnetic interaction ($J_1 > 0$) for the intralayer part, and a weak magnetic interlayer interaction of an A-AFM character for the interlayer regime. The previous results as we have found based-on the ED, and ELF. According to the number of exchange paths, it has been determined that $J_2 \sim 3J_3$ [12] in which, J_2 and $J_3 < 0$. Based-on that, we have analyzed the O–M distance and the M–O–M angle (that directly affect the J_1 exchange constant). Additionally, the O–O and the M–M interlayer distances, that have influence on J_2 and J_3 constants were also analyzed. This with the aim to understand the magnetic interaction as a function of M-transition metal cation. From Figure 4, we can see a substantial decrease on the O–M distance that suggest an increase in the J_1 exchange constant and superexchange interaction. In contrast, the O–O interlayer distance, which leads to the J_2 interaction increases. Additionally, it can be

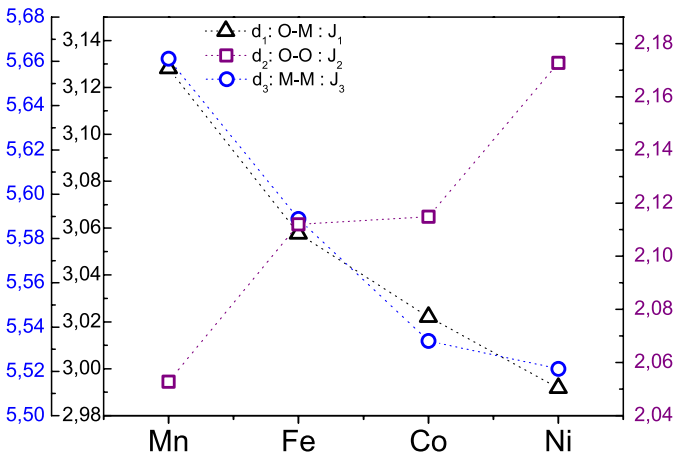

Figure 4. Interaction distances for β-M(OH)$_2$

seen that the M–M distances, related to the J_3 constant, decrease suggesting an increase of the J_3 from Mn to Ni. Although, this information is relevan in the analysis of the magnetic structure, further studies focused in the exact calculation of the exchange constants could confirmed the interactions observed in our work.

4. Conclusions

First-principles calculations were performed on the structural and magnetic properties of the M-based (M = Mn, Co, Fe, and Ni) hydroxides. An hexagonal structure with an A-AFM type ground state was found. Additionally, an important contribution of the Van der Waals interactions were observed in the c-axis direction. Finally, the magnetic ground state was explained in terms of the magnetic interactions and interatomic distances.

5. Acknowledgments

This work used the XSEDE which is supported by National Science Foundation grant number ACI-1053575. The authors also acknowledge the support from the Texas Advances Computer Center (with the Stampede2 and Bridges supercomputers). This work was supported by the DMREF-NSF 1434897, NSF OAC-1740111 and DOE DE-SC0016176 projects.

References

[1] Rall J, Seehra M and Choi E 2010 *Physical Review B* **82** 1–9

[2] Rall J D, Seehra M S, Shah N and Huffman G P 2010 *Journal of Applied Physics* **107** 09B511

[3] Norlund Christensen A and Olliver G 1972 *Solid State Communications* **10** 609–614

[4] Miyamoto H 1976 *Materials Research Bulletin* **11** 329–335

[5] Miyamoto H 1966 420–429

[6] Enoki T 1978 *Journal of the Physical Society of Japan*

[7] Kresse G and Furthmüller J 1996 *Physical review. B, Condensed matter* **54** 11169–11186

[8] Kresse G 1999 *Physical Review B* **59** 11–19

[9] Blochl P 1994 *Physical Review B* **50**

[10] Perdew J, Ruzsinszky A, Csonka G, Vydrov O, Scuseria G, Constantin L, Zhou X and Burke K 2008 *Physical Review Letters* **100** 1–4 ISSN 0031-9007

[11] Grimme S 2006 *Journal of computational chemistry* **16**

[12] Enoki, Tosiaki I T 1975 *Journal of the Physical Society of Japan* **39** 317–323

[13] Bantignies J, Deabate S and Righi A 2008 *The Journal of* **112** 2193–2201

[14] Murli C, Sharma S and Kulshreshtha S 2001 *Physica B: Condensed* **307** 111–116

[15] Hermet P, Gourrier L, Bantignies J L, Ravot D, Michel T, Deabate S, Boulet P and Henn F 2011 *Physical Review B* **84** 1–10

[16] Trevino P, Garcia-Castro A C, Lopez-Moreno S, Bautista-Hernandez A, Bobocioiu E, Reynard B, Caracas R and Romero A H 2018 *Phys. Chem. Chem. Phys.* **20**(26) 17799–17808